

Efficiency above the Shockley–Queisser Limit by Using Nanophotonic Effects To Create Multiple Effective Bandgaps With a Single Semiconductor

Zongfu Yu,^{*,†,‡} Sunil Sandhu,[†] and Shanhui Fan[†]

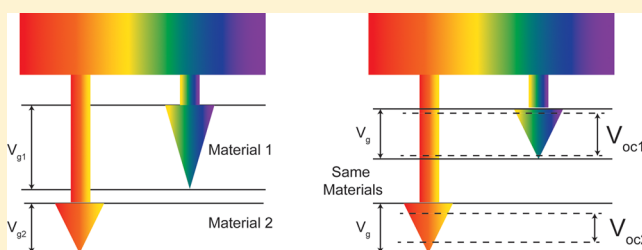
[†]Department of Electrical Engineering and Ginzton Laboratory, Stanford University, Stanford, California 94305, United States

[‡]Department of Electrical and Computer Engineering, University of Wisconsin, Madison, Wisconsin 53706, United States

S Supporting Information

ABSTRACT: We present a pure photonic approach to overcome the Shockley–Queisser limit. A single material can show different effective bandgap, set by its absorption spectrum, which depends on its photonic structure. In a tandem cell configuration constructed from a single material, one can achieve two different effective bandgaps, thereby exceeding the Shockley–Queisser limit.

KEYWORDS: Photon management, nanostructured solar cells, Shockley–Queisser limit, light trapping, tandem solar cells



Ever since the seminal work of Shockley and Queisser,¹ there have been significant efforts aiming to overcome the Shockley–Queisser limit for solar energy conversion.² The vast majority of these works aim to use materials or devices with electronic properties that are significantly different from the single bandgap semiconductors assumed in the original Shockley–Queisser analysis. These include the commercially available approach of multijunction solar cells, which utilizes multiple semiconductors with different band gaps,³ as well as more exploratory approaches such as hot-electron cells,⁴ multiple exciting generations,^{5–7} and intersubband⁸ solar cells. In contrast to all these works, in this Letter we propose and analyze an alternative scheme for overcoming the Shockley–Queisser limit based purely on photonic engineering. We show that with proper use of nanophotonic concepts, one could in fact overcome the Shockley–Queisser limit with a single semiconductor without the need to alter the electronic properties.

As an illustration we consider the structure shown in Figure 1, where both the top and bottom cells are made of the same semiconductor material and, therefore, have the identical electronic bandgap. However, they exhibit different effective bandgap due to their different absorption and emission spectra. We show that by controlling the top cell’s radiative emission through proper photonic design, the efficiency of such a single-material tandem cell can exceed the Shockley–Queisser limit. Related to our work here, it was recently shown that the open-circuit voltage of a cell can be enhanced by engineering its thermal emission.^{9–11} References 9–11, however, are still fundamentally constrained by the Shockley–Queisser limit.

To overcome the Shockley–Queisser limit, we need to reduce the thermalisation loss $\hbar\omega - V$. The voltage output V of a solar cell is more directly related open circuit voltage V_{oc}

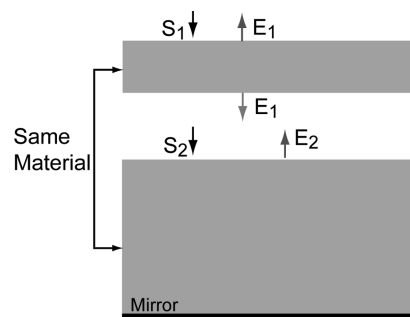


Figure 1. A tandem cell using a single electronic bandgap material. S_1 (S_2) is the incident sunlight absorbed by the top (bottom) cell. E_1 (E_2) is the emission of the top (bottom) cell.

rather than the electronic band gap of the material. Therefore, one can in fact regard the V_{oc} as the effective bandgap. We start our analysis by briefly reviewing the physics of open-circuit voltage V_{oc} in the detailed balance analysis. In an ideal solar cell without nonradiative processes, carriers are generated through sunlight absorption and depleted by radiative recombination. For a cell operating at the open-circuit condition, the net change of its carrier density is zero. Thus, at open circuit the radiative recombination rate is equal to the sunlight absorption rate. On the other hand, the radiative recombination rate is given¹ by $\exp(V_{oc}/k_B T)E$, where E is the thermal emission rate when the cell is in thermal equilibrium and has zero voltage, k_B is the Boltzmann constant, and T is the temperature of the cell.

Received: August 18, 2013

Revised: November 15, 2013

Published: November 26, 2013

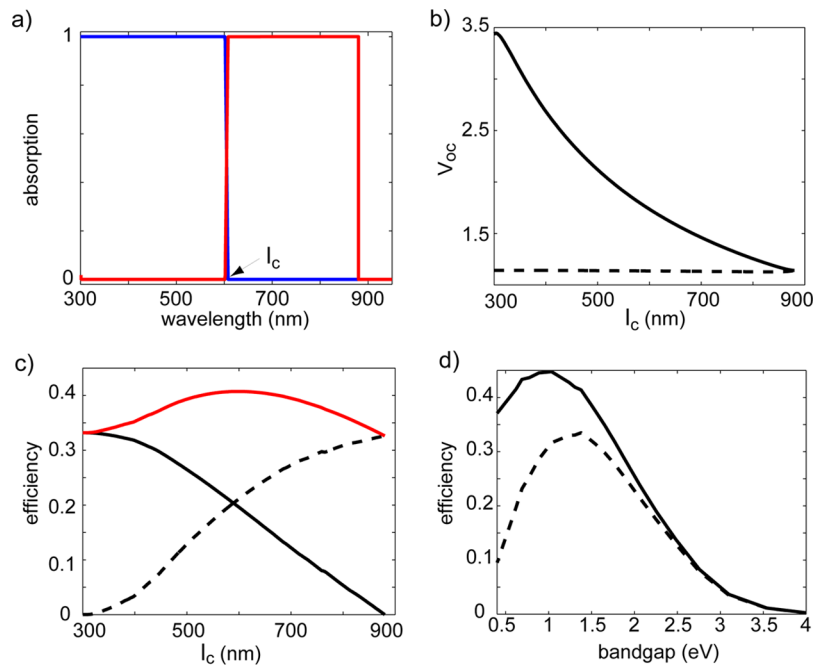


Figure 2. (a) The absorption spectra of the top cell (blue) and bottom cell (red) with an ideal cutoff wavelength λ_c , when the cells are placed in the tandem configurations shown in Figure 1. The electronic bandgap is at 880 nm. (b) The open-circuit voltage of the top (solid) and bottom (dashed) cells as a function of λ_c . Both cells are operating at open-circuit. (c) The efficiency of the top cell (solid black), the bottom cell (dashed black) and the total efficiency of the tandem cell (red) as a function of λ_c . (d) The limiting total efficiency of a two-junction cell as a function of its electronic bandgap energy (solid line). Dashed line indicates the Shockley–Queisser limit of a single-junction cell.

Here, below we will use thermal emission and radiative recombination interchangeably, referring to the same emission due to interband transitions. One can therefore increase the V_{oc} by reducing the thermal emission rate E , or equivalently, by reducing the emissivity of the cell.^{9–11}

For a single-junction cell, the above process for enhancing the open-circuit voltage cannot lead to any absolute maximum efficiency improvement. The Kirchhoff's law of thermal radiation indicates that the absorptivity of the cell must be equal to its emissivity. Thus, reducing the thermal emissivity necessarily comes at a cost of reducing the incident light absorption and, hence, a reduction of the cell's short-circuit current. As a result, no single-junction cell can go beyond the Shockley–Queisser limit. However, here we show that engineering of thermal emission can in fact be beneficial in terms of absolute maximum efficiency if one adopts a tandem cell configuration, even if the multiple junctions of the tandem cell use the same material with the same electronic bandgap.

As an illustration we consider a two-junction tandem cell consisting of only one material with one electronic bandgap at $\hbar\omega_g$ (Figure 1). The top cell is thin and does not absorb all the incident sunlight, while the bottom cell is thick and absorbs all the above-bandgap incident sunlight that passes through the top cell. The bottom cell also has a back mirror. Perfect antireflection is assumed at all interfaces. To highlight the main physics, we assume throughout the paper that both cells have angle-independent absorption coefficients, although the effects of angle dependency in absorptivity can be straightforwardly incorporated into our formalism. We also initially neglect all solar cell nonidealities including nonradiative recombination. The effect of adding such nonidealities into our analysis will be discussed toward the end of the paper.

The current–voltage relations of the two-junction tandem cell can be obtained by balancing the carrier generation and depletion in each cell (Figure 1):

$$\int_{\omega_g}^{\infty} S_1(\omega) d\omega + \int_{\omega_g}^{\infty} E_2(\omega, V_2, T) A(\omega) d\omega = 2 \int_{\omega_g}^{\infty} E_1(\omega, V_1, T) d\omega + I_1 \quad (1)$$

$$\int_{\omega_g}^{\infty} S_2(\omega) d\omega + \int_{\omega_g}^{\infty} E_1(\omega, V_1, T) d\omega = \int_{\omega_g}^{\infty} E_2(\omega, V_2, T) d\omega + I_2 \quad (2)$$

Equations 1 and 2 describe the top and bottom cells, respectively. The left- and right-hand sides of each equation describe the generation and depletion processes, respectively, with I_1 (I_2) being the current extracted from the top (bottom) cell, and V_1 (V_2) being the voltage across the top (bottom) cell. In eq 1, the first term on the left-hand side describes carrier generation due to solar radiation absorption:

$$S_1(\omega) = S_0(\omega) A(\omega) \quad (3)$$

where $S_0(\omega)$ is the incident sunlight's spectral photon flux density, which we assume in this letter to be the AM 1.5 global spectrum standard. $A(\omega)$ is the absorption spectrum of the top cell. The second term in the left-hand side of eq 1 describes the carrier generation due to the absorption of thermal radiation from the bottom cell. Here we assume that above the bandgap ω_g , the bottom cell has unity absorption for all angles and, thus, a unity emissivity. The emission of the bottom cell is given by

$$E_2(\omega, V_2, T) = H(\omega - \omega_g) \exp\left(\frac{qV_2}{k_B T}\right) \frac{\omega^2}{4\pi^2 c^2} \frac{1}{e^{\hbar\omega/k_B T} - 1} \quad (4)$$

where $H(\bullet)$ is the Heaviside step function, and c is the speed of light in vacuum. On the right-hand side of eq 1, the first term describes the carrier depletion due to thermal emission from the top cell, which we assume to emit symmetrically to both its top and bottom sides. The top cell's thermal emission into each side is

$$E_1(\omega, V_1, T) = H(\omega - \omega_g) \exp\left(\frac{qV_1}{k_B T}\right) \frac{\omega^2}{4\pi^2 c^2} \frac{1}{e^{\hbar\omega/k_B T} - 1} A(\omega) \quad (5)$$

where we have used Kirchoff's law¹² to relate the cell's emission to its absorption coefficient (i.e., $A(\omega)$).

The terms in eq 2 are interpreted similarly as that of eq 1. The first term in the left-hand side describes the bottom cell's absorption of the remaining portion of the incident sunlight that is transmitted through the top cell

$$S_2(\omega) = S_0(\omega)(1 - A(\omega))H(\omega - \omega_g) \quad (6)$$

The second term in left-hand side of eq 2 describes the bottom cell's carrier generation due to the absorption of thermal emission from the top cell. On the right-hand side of eq 2, the first term describes the carrier depletion due to thermal emission from the bottom cell, and the second term describes the current extracted.

Equations similar to eqs 1–6 have been used in the analysis of a conventional tandem cell.¹³ Here the difference in our design is that all junctions within our tandem cell have the same electronic bandgap. We use these equations to analyze the performance of the two-junction tandem cell shown in Figure 1. The limiting efficiency is obtained by optimizing $I_1 V_1 + I_2 V_2$, subject to the constraint described by eqs 1–6. We note that such a limiting efficiency assumes that both junctions output power independently.¹³ For concreteness, we take $\lambda_g = 2\pi c/\omega_g = 880$ nm, which corresponds to the bandgap wavelength of GaAs.

To understand the upper limit of performance, we start with an idealized absorption spectrum of the top cell $A(\omega) = H(\omega - \omega_c)$ with a cutoff wavelength $\lambda_c \equiv 2\pi c/\omega_c$ (Figure 2a), which prohibits all thermal emission at wavelengths longer than λ_c . Solving eqs 1–6, we see that a shorter λ_c leads to a higher voltage across the top cell, while the voltage across the bottom cell does not vary significantly with λ_c (Figure 2b). When the cutoff wavelength is at 600 nm, the tandem cell has an efficiency of 40.7%, which is much higher than the 33.2% Shockley–Queisser efficiency limit of a single-junction cell that uses the same bandgap material.

In the above idealized situation, the limiting efficiency of our tandem cell design (Figure 1) is the same as a tandem cell consisting of two materials with different bandgaps: the top and bottom cells having a bandgap at 600 nm and 880 nm, respectively.¹³ Therefore, we have shown that in order to achieve the efficiency benefits of a multijunction tandem cell, one need not use materials with different electronic bandgaps. Instead, it is sufficient to just have the capability of controlling the thermal emission of the top cell. Unlike electronic bandgaps, the emissivity or absorptivity of a cell is not an intrinsic property of a material, but rather can be controlled via photonic design. Therefore, our calculations indicate the

potential of photonic design to create a single electronic bandgap tandem cell.

As a realistic implementation of our single bandgap tandem cell design, we next show that one can indeed exceed the Shockley–Queisser limit with a GaAs tandem cell in slab geometry. We initially consider a top cell with a thickness of 300 nm and a bottom cell having sufficient thickness to absorb all the above-bandgap incident sunlight. In order to simplify the analysis, we assume that the top and bottom GaAs cells are separated by a distance larger than the optical wavelength, which ensures that no near-field coupling of thermal emission occurs between the two cells. Also, quantum confinement effects are not significant in GaAs cell with thickness of 300 nm;¹⁴ we therefore use the bulk dielectric constant of GaAs for our analysis.

As we have noted above (Figure 2), in order to achieve efficiency beyond the Shockley–Queisser limit the top cell needs to have excellent absorption at short wavelength range while having its absorption and, hence, its thermal emission suppressed near the band gap. A top cell consisting of a simple GaAs thin film is sufficient to satisfy these requirements. As shown in Figure 3a, the intrinsic absorption coefficient of GaAs

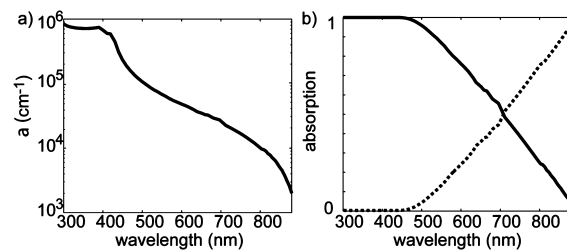


Figure 3. (a) Intrinsic absorption coefficient of GaAs. (b) Absorption spectra of the top cell (solid line) and the bottom cell (dashed line) when the two cells are placed in the tandem configuration shown in Figure 1. The top cell consists of a GaAs film with a thickness of 300 nm.

varies by 3 orders of magnitude from 300 nm to its band gap wavelength of 880 nm.¹⁵ The solid line in Figure 3b shows the absorption spectrum of a top cell consisting of a 300 nm thick GaAs thin film, calculated using the intrinsic absorption data in Figure 3a. Such a top cell does indeed exhibit both a strong absorption in the short wavelength range and a suppressed thermal emission near the band gap, satisfying the requirements above for the top cell.

By substituting the absorption profiles (Figure 3b) of both cells into eqs 1–6 we obtain a top cell's open-circuit voltage of 1.174 V, which is higher than the 1.14 V open-circuit voltage of a single-junction bulk GaAs cell. The bottom cell's open-circuit voltage is 1.133 V. The limiting efficiency of the two-junction tandem cell is 33.74%, which is noticeably higher than the 33.2% Shockley–Queisser efficiency limit of a single-junction GaAs solar cell under direct sun light. It is also higher than the 33.5% Shockley–Queisser efficiency limit^{1,16} of any single-junction cell under direct sun light. Thus, even the relatively simple geometry of a two-junction GaAs tandem cell is sufficient to achieve efficiencies beyond the Shockley–Queisser limit.

We next study the impact of the top cell's thickness on the tandem cell's current–voltage performance (Figure 4). The tandem cell's total efficiency peaks at 33.74% when the top cell has a thickness of 300 nm (Figure 4a), assuming a four-terminal

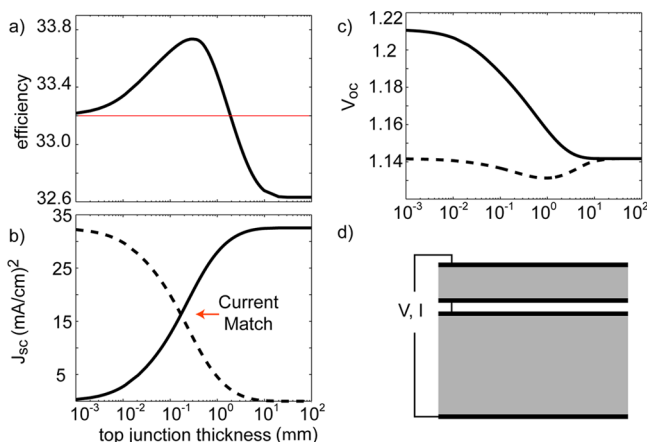


Figure 4. (a) The black line represents the total efficiency of the tandem cell as a function of top junction thickness. The red line is the Shockley–Queisser efficiency limit of a single-junction GaAs cell; (b) short-circuit current and c) open-circuit voltage of the tandem cell. Solid (dashed) line is for the top (bottom) cell. (d) Serial connection of two junction cells.

connection where each cell output independently. For serial connection (Figure 4d), we can choose the top cell to have a thickness of 160 nm in order to achieve current matching (Figure 4b). Both cells have a current of 16.63 mA/cm². The open circuit voltage of a serially connected cell is 2.317 V. The maximum efficiency is 33.71%. Therefore, with a two-terminal serial connection one can achieve nearly the same theoretical efficiency as the four-terminal case. The behavior of this total efficiency can be understood by analyzing the effect of the top cell's thickness on the current–voltage performance of each of the two cells. In general, as the top cell's thickness increases from zero, the top cell absorbs more of the incident sunlight and, consequently, the short-circuit current of the top cell increases while that of the bottom cell decreases (Figure 4b). Furthermore, we see that as the top cell's thickness decreases, its open-circuit voltage increases⁹ (Figure 4c) due to the reduced thermal emission near the bandgap.¹¹ On the other hand, the bottom cell's open-circuit voltage is not strongly influenced by the top cell's thickness because its thermal emission does not change as we vary the thickness of the top cell (Figure 4b).

When the top cell's thickness is reduced well below 300 nm, there is a significant reduction of incident sunlight absorbed by the top cell and, hence, its short-circuit current (Figure 4b) despite its voltage enhancement (Figure 4c). As a result, for the regime where the top cell's thickness is very small, the tandem cell's total efficiency is mainly determined by the bottom cell alone and approaches the 33.2% Shockley–Queisser efficiency limit of a single-junction GaAs cell when the top cell's thickness approaches zero (Figure 4a). On the other hand, when the top cell's thickness is more than 10 μm, the tandem cell's total efficiency is determined almost entirely by the top cell alone since the top cell absorbs almost all the incident sunlight. In this regime where the top cell's thickness is large, the total efficiency is around 32.63%, which is slightly lower than the single-junction Shockley–Queisser efficiency limit because of the top cell's bottom side emission.¹⁶ We emphasize that the efficiency of our GaAs tandem cell is above the Shockley–Queisser limit (red line in Figure 4a) as long as the top cell's thickness is below 1.9 μm. This wide range of the top cell's

thickness, where one can exceed the Shockley–Queisser limit, indicates the robustness of our approach.

The effect of adding nonradiative recombination can be added into the above analysis (see details in Supporting Information). The leading nonradiative recombination mechanism in GaAs is Auger recombination.^{17,18} For a top cell with 300 nm thickness this Auger recombination mechanism decreases the top cell's open-circuit voltage by less than 10^{−4} V. Therefore, there is negligible degradation in the tandem cell's total efficiency.

As shown above, a two-junction GaAs tandem cell using simple a slab geometry already exceeds the Shockley–Queisser limit. However, the performance of such a two-junction tandem cell is significantly lower than the ideal case shown in Figure 2, since the top cell exhibits only a limited absorption coefficient contrast between the long and short wavelength ranges. Nevertheless, a more sophisticated photonic design should be able to enhance the efficiency toward the ideal case in Figure 2 by both enhancing the short-wavelength absorption and suppressing the long-wavelength absorption in the top cell. For example, we can improve the voltage of the top cell by placing between the two cells a frequency-selective mirror,^{19,20} which only reflects light in the shorter wavelength range.

Alternatively, in the top cell one could apply a frequency-selective light-trapping technique²¹ in order to enhance light absorption in a selected spectral range. Unlike the thin film case shown in Figure 1, where there exist guided modes in the film that do not couple to the external radiation, the use of light-trapping ensures that all modes in the structure can couple to the external radiation, leading to absorption enhancement. The light-trapping enhancement ratio is determined by the optical density of states (DOS),^{22,23} which can be tailored to exhibit strong spectral dependence. By having high and low DOS in short and long wavelength ranges, respectively, light trapping can enhance the absorption contrast and thus the operation voltage of the top cell. An improvement of almost two percentage points can be achieved with an ideal light-trapping design (see Supporting Information).

Finally, our findings are also fully consistent with ref 16 regarding the importance of quantum yield. In this paper, we discuss the ideal limit of photovoltaic conversion efficiency. We have assumed the absence of nonradiative recombination, which is appropriate for the study of theoretical limit of solar cell. In such a case, the quantum yield is always 100%.

■ ASSOCIATED CONTENT

📄 Supporting Information

The effect of nonradiative recombination and using light trapping to enhance energy conversion efficiency. This material is available free of charge via the Internet at <http://pubs.acs.org>.

■ AUTHOR INFORMATION

✉ Corresponding Author

*E-mail: zyu54@wisc.edu.

📝 Notes

The authors declare no competing financial interest.

■ ACKNOWLEDGMENTS

This work is supported by the Department of Energy Grant DE-FG07ER46426, by the Department of Energy Bay Area Photovoltaics Consortium (BAPVC), and by the Global Climate and Energy Project (GCEP) of Stanford University.

■ REFERENCES

- (1) Shockley, W.; Queisser, H. J. *J. Appl. Phys.* **1961**, *32*, 510.
- (2) Green, M. A. *Third generation photovoltaics: advanced solar energy conversion*; Springer: New York, 2003.
- (3) King, R.; Law, D.; Edmondson, K.; Fetzer, C.; Kinsey, G.; Yoon, H.; Sherif, R.; Karam, N. *Appl. Phys. Lett.* **2007**, *90*, 183516.
- (4) Ross, R. T.; Nozik, A. J. *J. Appl. Phys.* **1982**, *53*, 3813.
- (5) Deb, S.; Saha, H. *Solid-State Electron.* **1972**, *15*, 1389.
- (6) Landsberg, P. T.; Nussbaumer, H.; Willeke, G. *J. Appl. Phys.* **1993**, *74*, 1451.
- (7) Nozik, A. J. *Physica E* **2002**, *14*, 115.
- (8) Luque, A.; Marti, A. *Phys. Rev. Lett.* **1997**, *78*, 5014.
- (9) Niv, A.; Gharghi, M.; Gladden, C.; Miller, O.; Zhang, X. *Phys. Rev. Lett.* **2012**, *109*, 138701.
- (10) Munday, J. N. *J. Appl. Phys.* **2012**, *112*, 064501.
- (11) Sandhu, S.; Yu, Z.; Fan, S. *Opt. Express* **2013**, *21*, 1209.
- (12) McMahan, H. O. *J. Opt. Soc. Am.* **1950**, *40*, 376.
- (13) De Vos, A. *J. Phys. D: Appl. Phys.* **1980**, *13*, 839.
- (14) Liang, D.; et al. *Adv. Energy Mater.* **2012**, *2*, 1254.
- (15) Palik, E. D. *Handbook of Optical Constants of Solids*; Elsevier Academic Press: Waltham, MA, 1985; Vol. 1, p 436.
- (16) Miller, O. D.; Yablonovitch, E.; Kurtz, S. R. *IEEE J. Photovoltaics* **2012**, *2*, 303.
- (17) Strauss, U.; Ruhle, W.; Kohler, K. *Appl. Phys. Lett.* **1993**, *62*, 55.
- (18) Kayes, B. M.; Nie, H.; Twist, R.; Spruytte, S. G.; Reinhardt, F.; Kizilyalli, I. C.; Higashi, G. S. *IEEE Photovoltaic Spec. Conf., 37th* **2011**, 4.
- (19) Hadipour, A.; Boer, B. D.; Blom, P. W. M. *J. Appl. Phys.* **2007**, *102*, 074506.
- (20) Bielawny, A.; Upping, J.; Miclea, P. T.; Wehrspohn, R. B.; Rockstuhl, C.; Lederer, F.; Peter, M.; Steidl, L.; Zentel, R.; Lee, S. M. *Phys. Status Solidi A* **2008**, *205*, 2796.
- (21) Yablonovitch, E. *J. Opt. Soc. Am. A* **1982**, *72*, 899.
- (22) Yu, Z.; Raman, A.; Fan, S. *Proc. Natl. Acad. Sci. U.S.A.* **2010**, *107*, 17491.
- (23) Yu, Z.; Fan, S. *Appl. Phys. Lett.* **2011**, *98*, 011106.